J Comput Aided Mol Des (2011) 25:743–752
DOI 10.1007/s10822-011-9455-8

In silico identification of new ligands for GPR17: a promising therapeutic target for neurodegenerative diseases

Ivano Eberini · Simona Daniele · Chiara Parravicini · Cristina Sensi · Maria L. Trincavelli · Claudia Martini · Maria P. Abbracchio

Received: 31 January 2011 / Accepted: 28 June 2011 / Published online: 9 July 2011

Abstract GPR17, a previously orphan receptor responding to both uracil nucleotides and cysteinyl-leukotrienes, has been proposed as a novel promising target for human neurodegenerative diseases. Here, in order to specifically identify novel potent ligands of GPR17, we first modeled in silico the receptor by using a multiple template approach, in which extracellular loops of the receptor, quite complex to treat, were modeled making reference to the most similar parts of all the class-A GPCRs crystallized so far. A high-throughput virtual screening exploration of GPR17 binding site with more than 130,000 lead-like compounds was then applied, followed by the wet functional and pharmacological validation of the top-scoring chemical structures. This approach revealed successful for the proposed aim, and allowed us to identify five agonists or partial agonists with very diverse chemical structure. None of these compounds could have been expected 'a priori' to act on a GPCR, and all of them behaved as much more potent ligands than GPR17 endogenous activators.

Keywords Molecular modeling · High throughput screening · Computational biology · Pharmacology · Drug discovery

Ivano Eberini, Simona Daniele, Chiara Parravicini equally contributed to this work.

Electronic supplementary material The online version of this article (doi:10.1007/s10822-011-9455-8) contains supplementary material, which is available to authorized users.

I. Eberini (✉) · C. Sensi
Gruppo di Studio per la Proteomica e la Struttura delle Proteine, Dipartimento di Scienze Farmacologiche, Università degli Studi di Milano, Via Giuseppe Balzaretti 9, 20133 Milano, Italy
e-mail: ivano.eberini@gmail.com

C. Parravicini · M. P. Abbracchio
Laboratorio di Farmacologia Molecolare e Cellulare della Trasmissione Purinergica, Dipartimento di Scienze Farmacologiche, Università degli Studi di Milano, Via Giuseppe Balzaretti 9, 20133 Milano, Italy

S. Daniele · M. L. Trincavelli · C. Martini
Dipartimento di Psichiatria, Neurobiologia, Farmacologia e Biotecnologie, Università degli Studi di Pisa, Via Bonanno Pisano 6, 56126 Pisa, Italy

Introduction

The seven-helix transmembrane G protein-coupled receptor (GPCR) family, encompassing more than 1,000 putative members, is crucially involved in cell-to-cell communication, in the response to environmental factors and hormones, and in the regulation of key cellular functions such as growth, differentiation and death. Due to such central roles, it is not surprising that malfunctioning of GPCRs (or of their signaling cascades) is associated to disease. A large majority of currently marketed drugs (including widely utilized anti-hypertensive, anti-thrombotic, anti-psychotic, anti-asthmatic and anti-ulcer drugs) indeed act through GPCRs, and have profoundly changed the medical approach to disease as well as patients' life quality and expectance. On this basis, the solution of GPCR atomistic structure has become a keystone for our understanding of their mechanism of action at a molecular level, and for the rational design and development of new therapeutic approaches that target these receptors.

The availability of crystallographic structures for some GPCRs in the RCSB Protein Data Bank allows collecting several structural data on this family. For many years, the only high-resolution GPCR structure was that of bovine rhodopsin (*b*Rh) [1], a member of the 7-helix transmembrane receptor/G-protein coupled receptor 1 family, opsin

subfamily, that has been solved in its *holo* form covalently bound to the inverse agonist retinal; thus, only *b*Rh could be used as the reference template in in silico comparative modeling. Recently, thanks to protein engineering, new GPCR structures of the same family have become available: the human adenosine A_{2A} receptor ($hA_{2A}R$) [2], the human β_2-adrenergic receptor ($h\beta_2AR$) [3–6], the turkey β_1-adrenergic receptor ($t\beta_1AR$) [7], and squid Rh [8]. Finally, also the structure of the *apo* form of the GPCR opsin has been solved [9]. While we were finalizing this manuscript, two further GPCR crystallographic structures have been published: the human dopamine D_3 receptor (hD_3R) and the human CXC chemokine receptor type 4 (CXCR4) [10, 11].

The availability of new structures allows a more accurate modeling for Rh-like receptors. In the past, the in silico homology modeling of GPCRs using *b*Rh as template, followed by high throughput screening of chemical databases and experimental validation, has almost exclusively led to the identification of pharmacological entities acting as antagonists or inverse agonists [12]. It is thus evident that the GPCR models obtained by this procedure are intrinsically affected by biases related to the selected template structure; more accurate models are likely to be obtained by using different templates for modeling each specific part of the selected GPCR.

Among all GPCRs, we have recently focused our attention on GPR17, a previously "orphan" receptor located at intermediate phylogenetic position between known purinergic P2Y and cysteinyl-leukotrienes (cysTLs) receptors (CysLTRs). Already characterized P2Y receptors and CysLTRs are activated, respectively, by extracellular nucleotides [13] or cysLTs [14], two distinct families of inflammatory molecules acting as "danger signals", that sense damage in tissues and activate local reparative processes. These endogenous signalling molecules and their receptors mediate immune responses and ischemic/inflammatory conditions, including stroke and several currently incurable neurodegenerative diseases. Interestingly, the "deorphanization" of GPR17 has demonstrated that this receptor indeed responds to both uracil nucleotides and cysLTs [13, 15, 16].

By employing a variety of in vivo rodent models of acute and chronic nervous system degenerative disorders, we and others [17–19] have recently validated GPR17 as a novel interesting target for the design of new drugs of potential use in human diseases characterized by neuronal and myelin dysfunction, including stroke, brain and spinal cord trauma and multiple sclerosis. However, all the published experimental data on GPR17 have been obtained using already available agonists and, in most cases, antagonists that have been purposely developed for other GPCRs (specifically, for the other well known P2Y or CysLTRs).

Here, to identify new and potent GPR17 ligands, we implemented the following strategy: (i) the in silico modeling of this GPCR based on the use of multiple templates; (ii) the in silico screening of virtual chemical libraries containing a large variety of molecules, including very diverse chemical structures that are totally unrelated to those already known to interact with either P2Y or CysLT receptors; (iii) the in vitro wet validation of the predicted pharmacological activity in a well established functional assay.

This approach has allowed us to successfully identify five candidate agonist or partial agonist molecules, belonging to very different chemical classes, able to modulate GPR17 activity with higher potency and efficacy than the endogenous reference compounds. This represents the first step towards the rational identification of candidate molecules for the development of entirely novel drugs for demyelinating and ischemic diseases, for which no effective therapy is yet available.

Methods

Comparative modeling

The human GPR17 sequence was downloaded from the UniProt—Protein Knowledgbase database [entry Q13304 (GPR17_HUMAN)]. Starting from its short isoform, a model was built based on multiple templates. We selected, among the 7-helix transmembrane receptor/G-protein coupled receptor 1 family, in addition to the sequences of proteins whose crystallographic structures are available, the sequences which present two conserved pairs of cysteines involved in putative disulphide bridges: one linking the extracellular loop (EL) 2 to transmembrane helix (TM) 3, the other connecting N-terminus with EL3. This subgroup includes members of the P2Y, CysLT, AGT, and chemokine (CCR, CXCR, CCRL, XCR, CX3CR) receptor families together with APJ, EBI2, GP174, GPR4, GP132, SPR1, G109A, G109B, GP171, GPR31, GPR34, GPR81, $P2RY_5$, $P2RY_9$, and $P2Y_{10}$ receptors. For all these sequences a global alignment based on CLUSTALW algorithm [20] has been produced and set as reference alignment for all the homology modeling procedures. Among the available GPCRs crystals, *b*Rh resulted to be the template with the highest CLUSTALW alignment score with respect to GPR17 (please, see Table S1). Accordingly, the TM regions of our model were built using *b*Rh TM domains (pdb 1U19).

In addition, the sequences of the available templates (*b*Rh, the $h\beta_2AR$, $t\beta_1AR$ and the $hA_{2A}R$) were compared with GPR17 through the Basic Local Alignment Search Tool algorithm optimized for protein alignment (BLASTP)

with the BLOSUM62 matrix. To model more accurately the less conserved extracellular and intracellular domains, we searched the BLAST alignments for: 1) absence/shortest extension of gaps, and 2) highest number of identical and/or conserved residues in the local alignments. Furthermore, secondary structure prediction programs were applied to GPR17 (please, see Results and Discussion), and compared the predictions for ILs and ELs to the experimental structures in the selected templates. On this basis, other templates were found more appropriate than *b*Rh to model some non-TM domains: human β_2AR was used to build EL1 and IL2 (pdb 2RH1), $t\beta_1$AR (2VT4) for EL2 and A_{2A}R (3EML) for EL3.

All the comparative modeling procedures were carried out with the Homology module of the Molecular Operating Environment 2008.10 (MOE). The alignment produced by the Align program of MOE with default parameters was manually adjusted according to BLAST outputs.

Comparative model building was carried out with the MOE Homology Model program. 1U19 was set as primary template, and the option 'Use Selected Residues to Override Template(s)' was checked in order to override the primary template with the more appropriate ones only for the selected residues. Ten independent models were built and refined, and then the highest scoring intermediate model was submitted to a further round of energy minimization (EM). Both for the intermediate and the final structures the refinement procedures consisted in EM runs based on the AMBER99 force field, with the reaction field solvation model.

The two disulfide bonds, between cysteines 23 and 269, and between 104 and 181, were created through the MOE Builder module. The ELs were then submitted to energy minimization runs, after fixing TMs and ILs. Six EM runs, all down to an RMS gradient of 0.5 kcal/mol Å, were carried out while restraining the ELs atoms with a quadratic force from 10^5 down to 10^{-1} kcal/mol Å^2. A further EM run was carried out without any restraint down to an RMS gradient of 0.5 kcal/mol Å.

The quality of the final model was carefully checked with the MOE Protein Geometry module to make sure that the stereochemical quality of the proposed structure was acceptable.

Binding site analysis

The GPR17 binding site was identified through the MOE Site Finder module, which uses a geometric approach to calculate possible binding sites in a receptor starting from its 3D atomic coordinates. This method is based not on energy models but on alpha spheres, which are a generalization of convex hulls [21].

Molecular database preparation

The Asinex Platinum Collection (http://www.asinex.com/download-zone.html) is a lead-like structural library containing approx. 130,000 in-house synthesized compounds. The SD file containing all the structures was downloaded and the MOE Conformation Import module was run on this file to produce a single low-energy conformation for each putative ligand contained in the Asinex SD file.

Molecular docking

The in silico screening was carried out with the Dock program contained in the MOE Simulation module. The full GPR17 structure was set as Receptor. Before starting with the placement procedure, 1,000 conformations were generated for each ligand by sampling their rotable bonds. The selected placement methodology was Triangle Matcher, in which the poses are generated by superposing triplets of ligand atoms and triplets of receptor site points. The receptor site points are alpha spheres centers that represent locations of tight packing. Before scoring all the generated poses, duplicate complexes were removed. Poses are considered as duplicates if the same set of ligand-receptor atom pairs are involved in hydrogen bond interactions and the same set of ligand atom receptor residue pairs are involved in hydrophobic interactions. The accepted poses were scored according to the London dG scoring, which estimates the free energy of binding of the ligand from a given pose.

$$\Delta G = c + E_{flex} + \sum_{h-bonds} c_{HB} f_{HB} + \sum_{m-lig} c_M f_M + \sum_{atoms\_i} \Delta D_i \quad (1)$$

where c represents the average gain/loss of rotational and translational entropy; E_{flex} is the energy due to the loss of flexibility of the ligand (calculated from ligand topology only); f_{HB} measures geometric imperfections of hydrogen bonds and takes a value in [0,1]; c_{HB} is the energy of an ideal hydrogen bond; f_{M} measures geometric imperfections of metal ligations and takes a value in [0,1]; c_{M} is the energy of an ideal metal ligation; and D_i is the desolvation energy of atom i. The difference in desolvation energies is calculated according to the formula

$$\Delta D_i = c_i R_i^3 \left\{ \iiint_{u \notin A \cup B} |u|^{-6} du - \iiint_{u \notin B} |u|^{-6} du \right\} \quad (2)$$

where A and B are the protein and/or ligand volumes with atom i belonging to volume B; R_i is the solvation radius of atom i (taken as the OPLS-AA van der Waals sigma parameter plus 0.5 Å); and c_i is the desolvation coefficient of atom i. The coefficients $\{c, c_{HB}, c_M, c_i\}$ have been fitted from approx. 400 x-ray crystal structures of protein–ligand complexes with available experimental pK_{i} data. Atoms are

categorized into about a dozen atom types for the assignment of the c_i coefficients. The triple integrals are approximated using Generalized Born integral formulas.

Only the top scoring solution was kept and submitted to a further refinement step, based on molecular mechanics (MM). In order to speed up the calculation, residues over a 6 Å cutoff distance away from the pre-refined pose were ignored, both during the refinement and in the final energy evaluation. All receptor atoms were held fixed during the refinement. During the course of the refinement, solvation effects were calculated using the reaction field functional form for the electrostatic energy term. The final energy was evaluated using the MMFF94x forcefield with the Generalized Born solvation model (GBIV) [22].

All the ligands contained in the Platinum library were screened according to the above procedure. The 15 top scoring compounds were resubmitted to the same docking procedure, keeping for each one of them 300 poses. The 5 ligands associated with the lowest energy scores (more favorable poses) were bought from Asinex and tested by in vitro pharmacology experiments.

The estimated binding affinity and the ligand efficiency were calculated through the MOE LigX module. The pK_i was computed through the binding free energy estimated with the London dG scoring function.

Protein ligand interaction fingerprints (PLIF)

PLIF is a method for summarizing the interactions between ligands and proteins using a fingerprint scheme. Hydrogen bonds, ionic interactions, and surface contacts are classified according to the residue of origin, and built into a fingerprint scheme that is representative of a given database of protein–ligand complexes. All the 300 poses for the 5 selected compounds were submitted to the MOE PLIF program in its default configuration, except for the non-specific surface contacts which have been disregarded, generating a barcode plot, summarizing the amino acid involvement in protein ligand interactions.

Cell culture and transfection

Human 1321N1 cells were cultured as described. For [^{35}S]GTPγS, 10^6 1321N1 cells were seeded on 75 cm^2 flasks and transfected, by the calcium phosphate precipitation method, with both the pcDNA3.1 vector containing the construct encoding for the human GPR17 receptor and the empty pcDNA3.1 vector as a control [23].

[^{35}S]GTPγS binding assay

Preliminary association kinetic studies performed in 1321N1 cells to define optimal binding conditions have already been published [15]. Control and transfected cells were homogenized in 5 mM Tris–HCl and 2 mM EDTA (pH 7.4) and centrifuged at 48,000 g for 15 min at 4 °C. The resulting pellets (plasma membranes) were washed in 50 mM Tris–HCl and 10 mM $MgCl_2$ (pH 7.4) and stored at −80 °C until used. Nucleotide-stimulated [^{35}S]GTPγS binding in membranes of cells expressing the human receptor was performed as described previously [13, 15, 23].

Statistical analysis

For the analysis and graphic presentation of [^{35}S]GTPγS binding data, a nonlinear multipurpose curve fitting computer program (Graph-Pad Prism) was used. All data are presented as the mean ± SEM of three different experiments. Data were tested for statistical significance with the paired Student's t test or by analysis of variance (one-way ANOVA), as appropriate. When significant differences were observed, the Newman-Keuls multiple comparison test (one-way ANOVA) was performed. A value of $p < 0.05$ was considered significant.

Results and discussion

Comparative modeling and binding site analysis

In the past, in silico models have been obtained for several pharmacological targets, including GPCRs, through comparative modeling based on the structure of *b*Rh [24, 25]. These models have been successfully exploited for the rational design of new drugs [26]. In the case of GPR17, the availability of four recently crystallized proteins of the same receptor family (see above) allowed us to select different templates for the discrete modeling of distinct parts of the receptor. The newer crystals, *h*D$_3$R and *h*CXCR4, could not be used, since they were not available at the moment of the modeling procedures. Table S1 reports the CLUSTALW score for the alignment between GPR17 and all the available GPCR crystals at the moment of GPR17 modeling; *b*Rh has the highest alignment score. Furthermore, a local alignment run through BLAST between GPR17 TM helices and the same motives of all the available templates confirmed that *b*Rh is indeed suitable as a primary template for modeling the 7 TM helices (data not shown).

Table S2 lists the alternative templates and reports the details of local alignments. These templates were selected for loop modeling according to the procedure reported in the Comparative Modeling paragraph of the Experimental Section. Table S2 reports the best local alignments for loops not modeled onto *b*Rh, selected according to the lowest number of gaps and the highest number of identical and conserved amino acids.

In detail, we devoted special attention to extracellular loop 2 (EL2). From the literature, it is well known that EL2 exerts an all-encompassing role acting as a gatekeeper and being involved in ligand recognition and allosteric modulation [27]. As accounted in great detail by Costanzi [25], modeling EL2 on *b*Rh structure consistently produces a conformation that buries the loop in the 7TM pocket. This makes it difficult to identify the binding site on the receptor and to carry out molecular docking simulations. Different approaches for solving this problem have been successfully proposed: the de novo building of EL2 [25] or the molecular mechanics refinement of EL2 built by homology to *b*Rh, as already published by our research group [28, 29]. The newly available GPCR structures show different loop arrangements, suggesting a very high local structural variability, likely connected to molecular recognition and selectivity mechanisms. Accordingly, to steer EL2 modeling we ran a secondary structure prediction on GPR17. First, we tested 4 different secondary structure prediction programs on the primary structure of $t\beta_1$AR and $h\beta_2$AR, and, only for the EL2, compared the results obtained from all these programs with the experimental crystallographic structure. PREDATOR [30, 31] and the MOE Predicted Secondary Structure program [32] correctly recognized the EL2 of $t\beta_1$AR and $h\beta_2$AR as containing a short helix, while the same loop in *b*Rh contains no helix. On the contrary, PSIPRED [33] and SSPRO [34] were not able to detect any helix content in EL2. For this reason, to predict the structure of EL2 in GPR17, we used PREDATOR and MOE Predicted Secondary Structure programs. The obtained local secondary structure was identical to that of $t\beta_1$AR and $h\beta_2$AR. Furthermore, our local alignments suggested that EL2 should be built using $t\beta_1$AR as template. Through this procedure, we obtained a non-buried EL2 that did not need any further refinement step.

Figure 1 shows the structural model of GPR17 we finally built; color-code shows the correspondence with the different templates. The analysis of GPR17 through the MOE Site Finder module revealed 13 putative binding sites; the top-scoring contained 339 potential contact atoms, among which 51 were hydrophobic and 245 involved sidechain atoms. This site (Fig. 1b, c) is localized in an extracellular region inside the ELs and close to the plasma membrane. The second putative binding site was characterized by a slightly lower score, but was located on the intracellular side of GPR17, so it was excluded, being totally inadequate for ligand binding. Correct identification of putative binding sites in transmembrane (TM) domain receptors by MOE Site Finder has already been thoroughly discussed in Globisch et al. [35].

Table S3 lists the amino acids of the top-scoring binding site according to their potential hydrophobic contacts. Several of the listed amino acids have already been proposed or

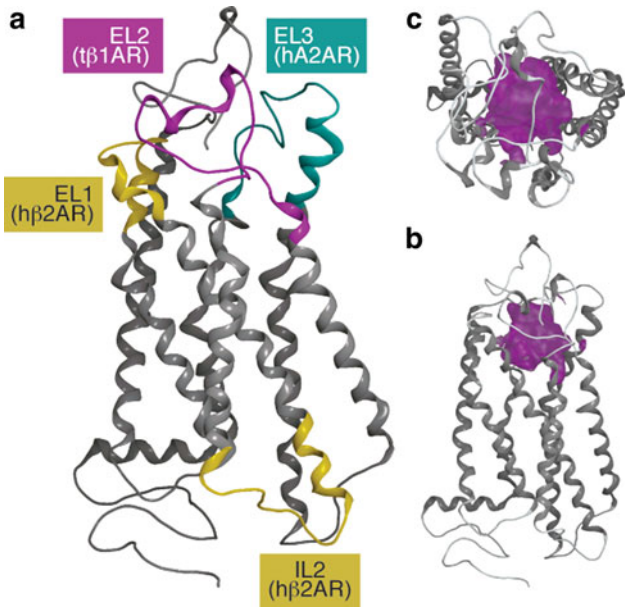

Fig. 1 **a** Structural model of GPR17 built as a chimera of four homology templates. Color code: *silver*, bovine rhodopsin; *gold*, human β_2-adrenergic receptor; *green*, human A_2 adenosine receptor; *purple*, turkey human β_1-adrenergic receptor. **b** and **c** Molecular surface of the binding site in the GPR17 model, *side* (**b**) and *top* (**c**) view

demonstrated to be involved in GPR17 ligand molecular recognition [28, 29]. The GPR17 binding site involves amino acids from different TMs and ELs, and several residues of EL2 seem to be crucial for the interaction.

A BLAST search in the UniProtKB/Swiss-Prot database for human proteins homologous to GPR17 found out 17 sequences with an approximately 30% identity and significant Z score values; search was limited to human proteins, in order to minimize redundancy. Table S4 reports the list of the identified proteins and the conserved amino acids of the binding site. Out of the 41 amino acids composing the GPR17 binding site, 3 are conserved in all the identified homologous proteins: Tyr90, Cys104, and Tyr116. Cys104 forms a disulfide bond with Cys181, which is highly conserved in this class of GPCRs. Seven amino acids (Tyr90, Cys104, Phe111, Tyr112, Tyr116, Tyr251, and Thr282) are conserved in at least 50% (>8) of the identified proteins. Except for Cys104 and Phe111, a hydroxyl functional group characterizes all these amino acids, which can be relevant in the formation of hydrogen bonds for the molecular recognition by the GPCRs.

Bondensgaard et al. [36] identified 3 privileged structures recognized by all class A GPCRs. The reported scaffolds have been described to interact with 35 highly conserved amino acids which could be sub-classified in two groups: (i) residues present in all class A GPCRs, mainly hydrophobic and/or aromatic, relevant for the molecular recognition mechanism between ligand and receptor, and,

(ii) variable residues responsible for the selectivity. Among these 35 amino acids, 12 are also conserved in the GPR17 binding site: Thr107, Gly108, Phe111, Tyr112, Tyr116, Leu166, His192, Ala193, Ser196, Tyr251, Arg255, Ser283.

Molecular docking

We carried out the docking procedure in two steps, screening and refinement. To evaluate the docking results in the screening step we made reference to molecular mechanics with the generalized Born solvation model (MM/GBIV) energy score, since Vilar et al. [37] have demonstrated that this was the best choice for virtual screening *versus* β_2AR, in the absence of a training set. Furthermore, scoring the poses according to the London dG function produced only results with a negative energy because this function does not take into account the van der Waals repulsive forces (not shown). In addition, since the refinement step is based on the MMFF94x forcefield, it was more consistent to score the poses according to the same parameters in both phases.

Figure S1 reports the MM/GBIV energy score for all the 300 poses of the 15 top-scoring ligands from the screening step. The 5 ligands whose poses scored at the lowest energy values were selected for the in vitro experiments. Table 1 reports some physico-chemical parameters for these ligands, for three well-known GPR17 agonists (UDP, UDP-glucose, UDP-galactose) and for two antagonists (MRS2179 and cangrelor). The reported pK_i (-Log dissociation constant) values are computed through the London dG scoring function. As already discussed by Eberini et al. [38–40], this and other empirical scoring functions are useful to rank the complexes according to their dissociation constant. The docking score of the poses according to the MM/GBIV and the pK_i values (affinities) computed through the London dG scoring function show a similar trend, suggesting that both these methods, based on different approaches, can be used to evaluate docking results and to compute approximate binding free energies for the systems under investigation.

Table 1 Physico-chemical parameters for the top-scoring ligands, and for selected GPR17 agonists and antagonists, after the refinement step of the docking procedure

Ligand	MM/GBIV docking score (kcal/mol)	Affinity (pK_i)	MW	Donor/acceptor
1	−18.4	10.5	460.6	1/5
2	−21.3	12.3	524.6	1/7
3	−20.9	12.7	535.6	4/6
4	−19.7	11.3	517.6	1/6
5	−19.7	11.4	531.9	2/6
UDP	−21.8	11.0	400.1	2/11
UDP-glucose	−28.4	15.5	565.3	8/16
UDP-galactose	−30.3	14.1	565.3	8/16
MRS2179	−24.0	10.9	421.2	1/12
cangrelor	−42.7	16.6	772.3	3/14

Figure 2 reports the 2D structures for the 5 top scoring compounds. They belong to different chemical classes, suggesting that this in silico screening allows identifying putative lead compounds that are not necessarily related to the already known ligands. This is a particularly important result, since none of the currently available GPR17 ligands, which are chemically related to ligands for already known P2Y and cysLT receptors, is indeed specific for GPR17.

Protein ligand interaction fingerprints (PLIF)

The PLIF barcode plot (Figure S2) reports all the poses from the docking refinement step for the 5 ligands submitted to in vitro pharmacology experiments. Thirty-one amino acids are recognized as relevant in the interaction between GPR17 and these compounds. All the residues positive to the PLIF analysis belong to the set of amino acids previously identified by the MOE Site Finder module. Site Finder did not recognize Glu187, identified as an interacting amino acid by PLIF. However this residue interacts with the ligands in a very low number of the 1444 selected poses, suggesting its marginal role in the recognition process. Tyr90, Thr107, Tyr112, Ala189, Tyr251, Arg273, and Ser283 are the residues associated with the highest number of interactions with the tested ligands. Interestingly, three tyrosine residues (Tyr90, Tyr112, and Tyr251) are among the most conserved within the set of residues relevant for GPR17 recognition mechanism. From the barcode plot (Figure S2), two compounds present a higher number of interactions with the receptor than the other three. Of these, ligand 3 has the greatest pK_i value, whereas ligand 3 behaves as a partial agonist in the molecular pharmacology experiments (please, see below). Furthermore, in previous papers from our research group [13, 28], by using a combination of different in silico and in vitro technical approaches, we demonstrated that one of the residues (R255) belonging to GPR17 binding site and singled out by the PLIF (Figure S2) plays a crucial role in ligand molecular recognition, since its mutation (R255I) is able to modify GPR17 function.

[^{35}S]GTPγS binding assay

In order to verify the reliability of the in silico predictions and to evaluate the functional activity on GPR17 of the selected compounds, the 5 candidate molecules were tested in a well established GPCR assay, the [^{35}S]GTPγS binding, based on the ability of agonists to increase the binding of

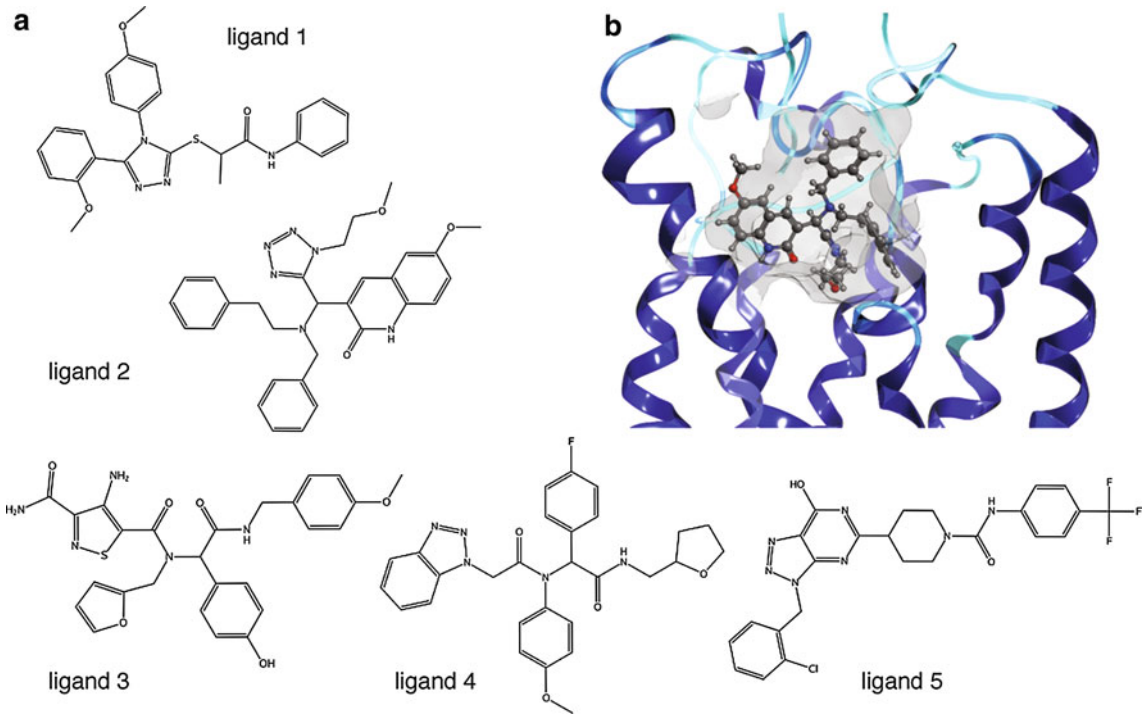

Fig. 2 **a** Chemical structures of the five top-scoring GPR17 ligands. **b** Lowest energy pose of ligand 2 interacting with GPR17 binding site

radioactive GTP to the activated GPCR. Antagonist activity was instead assessed through the ability to counteract the increase of [^{35}S]GTPγS binding induced by the model agonist LTC_4. [^{35}S]GTPγS binding results are reported in Fig. 3 and Table 2. All the 5 tested molecules showed a very high potency across a narrow range of concentrations: from sub-nanomolar to nanomolar range. Differences in ranking between molecular docking and data from the [^{35}S]GTPγS binding assay might be due to different causes, the most relevant being that computed pK_i refer only to the ligand::receptor free energy of binding, whereas [^{35}S]GTPγS binding assesses receptor activation. In this respect, it has to be emphasized that the [^{35}S]GTPγS assay utilized here not only verifies the ability of the tested compounds to interact with GPR17, but also measures their intrinsic activity (α), classifying them as agonists, partial agonists, or antagonists. It is therefore a functional assay that cannot be directly compared with the in silico molecular modeling method.

In the in vitro assays all the tested compounds, except ligand 5, showed an efficacy comparable to, or even higher than, that of the reference compound LTC_4. Only ligand 3 showed an efficacy significantly lower (89.6%) than that of LTC_4, suggesting that it could act as a partial agonist. However, the very high pK_i values (Table 1) computed for the two tested GPR17 antagonists (MRS2179 and cangrelor), suggested that our model is suitable also for the identification of ligands with $0 < \alpha < 1$. Despite all the 5 top-scoring tested compounds behave as full or partial agonists, from in silico data obtained on antagonists we believe that a further screening of the remaining top-scoring hits could also provide us with some antagonists. Figure 3a shows the concentration–response curves of the 5 tested compounds in the [^{35}S]GTPγS assay performed on 1321N1 cells expressing GPR17. LTC_4 was unable to induce any response in cell transfected only with the control vector pcDNA3.1 (black line), confirming that the increase of [^{35}S]GTPγS binding is mediated by the presence of GPR17.

In order to evaluate if the selected ligands bind to the same site on GPR17, we built concentration–response curves for the most potent compound in presence of different concentrations of cangrelor (Fig. 3c). The curves were shifted to the right (increased EC_{50}), but no effect was observed on the efficacy. This result suggests that cangrelor is a competitive antagonist for ligand 1, and that these two molecules compete for the same binding site on GPR17.

In Fig. 3b the antagonistic effect of cangrelor is tested on GPR17 activation induced by Asinex compounds. All these compounds are antagonized by cangrelor, a $P2Y_{12/13}$ and GPR17 antagonist, which is able to bind to the GPR17 uracil nucleotide-binding site [15].

The same experiment was repeated with montelukast, an antagonist of the CysLTR1 [41] (Fig. 3d). It has already been demonstrated that lukasts can act as inhibitors not only of CysLTR1, but also of GPR17 [15]. However, the concentration–response curves for ligand 1, obtained in the presence of montelukast, showed a reduction of the efficacy of ligand 1, suggesting a non-competitive antagonism,

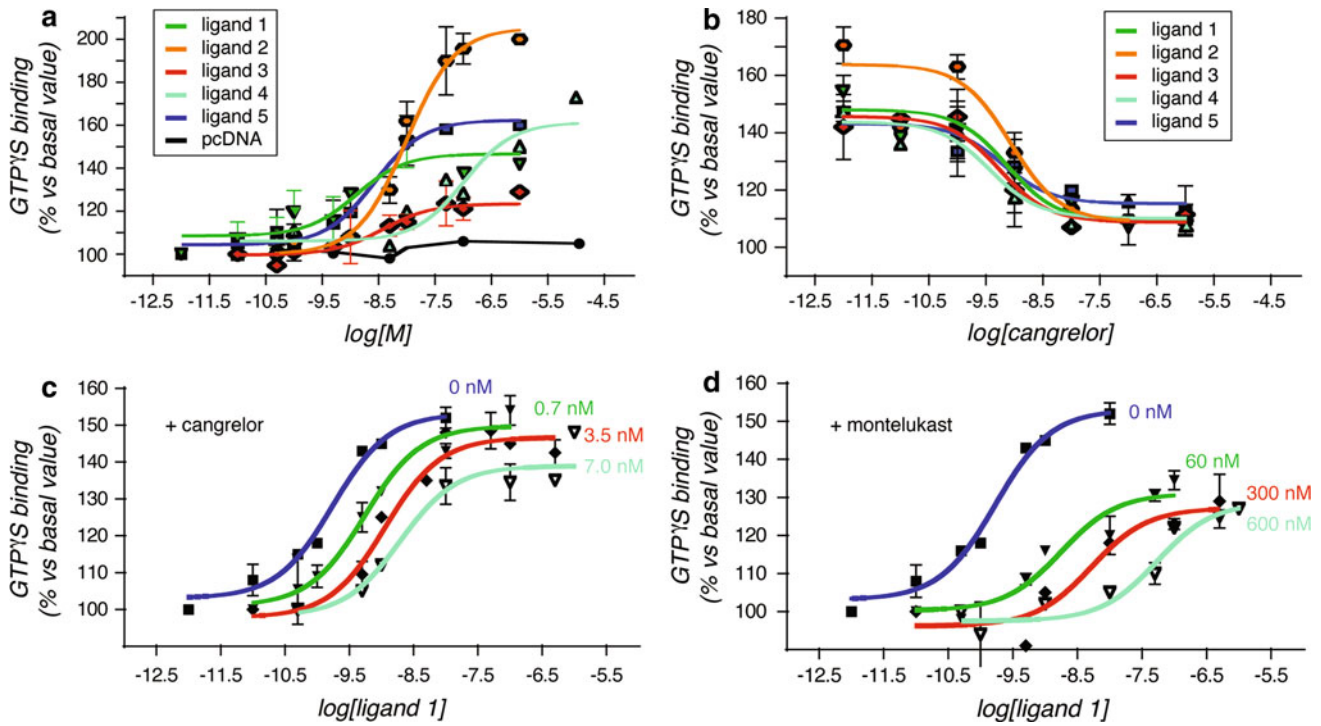

Fig. 3 [^{35}S]GTPγS binding assays on GPR17: **a** Concentration–response *curves* for the five top-scoring compounds selected through the in silico screening procedure. Membrane aliquots obtained from 1321N1 cells transfected with empty vector (control cells) or pcDNA3.1-*h*GPR17 were incubated with different Asinex compound concentrations. All data are expressed as percentages of basal [^{35}S]GTPγS binding (set to 100%) and are means SEM of 3 different experiments, each performed in duplicate. **b** Effect of the P2Y receptor antagonist cangrelor on agonist-stimulated [^{35}S]GTPγS binding. Membranes from pcDNA3.1-*h*GPR17-transfected cells were preincubated for 10 min with graded cangrelor (0.01 nM–1 μM) concentrations and then stimulated with a selected concentration for each Asinex ligand (10 fold over the EC_{50} value). All data are expressed as percentages of basal [^{35}S]GTPγS binding (set to 100%) and are means SEM of 3 different experiments, each performed in duplicate. Inhibition of agonist binding by purinergic or CysLT GPR17 antagonists in the [^{35}S]GTPγS binding assay: **c** Antagonistic activity of cangrelor on the stimulation of [^{35}S]GTPγS binding induced by ligand 1. Membranes from GPR17-expressing 1321N1 cells were incubated with ligand 1 (0.01–10 nM) in the absence or presence of graded antagonist concentrations as indicated. Binding of [^{35}S]GTPγS to G proteins was then quantified. **d** Antagonistic activity of montelukast on the stimulation of [^{35}S]GTPγS binding induced by ligand 1. Membranes from GPR17-expressing 1321N1 cells were incubated with ligand 1 (0.01–10 nM) in the absence or presence of graded antagonist concentrations as indicated. Binding of [^{35}S]GTPγS to G proteins was then quantified. All data are expressed as percentages of basal [^{35}S]GTPγS binding (set to 100%) and are means SEM of 3 different experiments, each performed in duplicate

Table 2 Pharmacological parameters for the tested compounds

Compound	EC_{50}	E_{max}	% Emax *versus* standard	IC_{50} compound *versus* cangrelor
ASN02563583 (1)	109 ± 28 pM	145.6 ± 5.7	100.6	0.64 ± 0.19 nM
ASN04421891 (2)	3.67 ± 0.51 nM	206.8 ± 8.3	142.8***	0.71 ± 0.09 nM
ASN04450772 (3)	1.18 ± 0.08 nM	129.7 ± 0.7	89.6***	0.51 ± 0.04 nM
ASN04885796 (4)	2.27 ± 0.07 nM	173.5 ± 0.5	119.8***	0.48 ± 0.17 nM
ASN06917370 (5)	268 ± 9 pM	161.5 ± 2.4	111.5**	0.78 ± 0.22 nM
LTC_4 100 nM		144.8 ± 0.4	100	

** $p < 0.01$ *versus* LTC_4 set to 100%

*** $p < 0.001$ *versus* LTC_4 set to 100%

probably exerted through an allosteric mechanism on a binding site different from that bound by uracil nucleotides. The evidence that purinergic and leucotrienic ligands do not share the same binding site on GPR17 had indeed already arisen from our previous data [15, 28].

Conclusions

Bovine Rh, which has been used as the unique template for GPCR modeling for several years, is not anymore the single crystallographic structure available for GPCRs.

Here, for GPR17 homology modeling, besides *b*Rh, we also took advantage of three recently crystallized GPCRs (i.e, $t\beta_1$AR, $h\beta_2$AR, and $hA_{2A}R$). Comparative modelling has produced a 3D structure with a well-defined binding site. No induced fit, molecular dynamics simulation or loop rebuilding procedures were necessary as a preliminary step to the molecular docking simulations. The most conserved part of GPR17 (TM helices) showed a slightly higher identity *versus* *b*Rh than *versus* other crystallized GPCRs (Table S1). However, this is not true for receptor loops, and especially for EL2 since, in *b*Rh, this element is buried inside the receptor binding site and has a β-hairpin structure. In class A GPCRs, ELs seem to play a key role in ligand molecular recognition and binding. This specificity advises against a de novo modeling approach. The increasing availability of new GPCR crystals, such as the recent *h*CXCR4 and hD_3R, will provide new templates for improving the quality of GPCR models.

The screening of 130,000 lead-like and non-targeted compounds allowed us to select a set of putative GPR17 ligands belonging to highly diverse chemical classes. The in vitro evaluation of a subset consisting of the 5 top-scoring compounds through a well-standardized functional assay fully confirmed the computational predictions obtained by applying a molecular modeling strategy to our specific aim: identifying new GPR17-targeting scaffolds. These ligands are the first examples of molecules acting at GPR17 that have not been developed/used as CysLTR1 or P2YR modulators. The molecular pharmacology experiments suggested that the selected compounds can bind to the GPR17 uracil binding site and can be competitively antagonized by cangrelor. Inhibition of ligand 1 maximal effect (efficacy) induced by montelukast suggests a non-competitive antagonism, which likely involves a binding site different from the site of interaction of uracil and cangrelor. Among the 5 tested ligands, we identified 4 full agonists, with a better potency than the reference ligand (LTC_4), and a partial agonist. Considering the dual role of GPR17 in promoting both damage and repair depending on specific times after the injury [19], the availability of a partial agonist could be very advantageous from a therapeutic point of view. In fact, during the acute phase of an ischemic event, when nucleotides and cysLTs are massively released at the inflammation site [42, 43], the activity of GPR17 can be finely tuned by a partial agonist by blocking the detrimental effects mediated by excessive and dysregulated receptor activation. On the other hand, by keeping the receptor partially activated during the subsequent ischemic phases, when nucleotides and cysLTs levels decrease, a partial agonist would not counteract the repair and trophic actions induced by these endogenous molecules.

Acknowledgments This work was partially supported by Progetti di Ricerca di Interesse Nazionale COFIN-PRIN 2008, Ministero dell'Istruzione dell'Università e della Ricerca "Purinoceptors and neuroprotection: focus on the new purinergic receptor GPR17" to MPA and MLT. CP is recipient of a Cariplo Foundation fellowship (*"Promuovere progetti internazionali finalizzati al reclutamento di giovani ricercatori"*, Project N. 2008.2907 to MPA).

References

1. Okada T, Sugihara M, Bondar AN, Elstner M, Entel P, Buss V (2004) J Mol Biol 342:571
2. Jaakola VP, Griffith MT, Hanson MA, Cherezov V, Chien EY, Lane JR, Ijzerman AP, Stevens RC (2008) Science 322:1211
3. Rasmussen SG, Choi HJ, Rosenbaum DM, Kobilka TS, Thian FS, Edwards PC, Burghammer M, Ratnala VR, Sanishvili R, Fischetti RF, Schertler GF, Weis WI, Kobilka BK (2007) Nature 450:383
4. Cherezov V, Rosenbaum DM, Hanson MA, Rasmussen SG, Thian FS, Kobilka TS, Choi HJ, Kuhn P, Weis WI, Kobilka BK, Stevens RC (2007) Science 318:1258
5. Rosenbaum DM, Cherezov V, Hanson MA, Rasmussen SG, Thian FS, Kobilka TS, Choi HJ, Yao XJ, Weis WI, Stevens RC, Kobilka BK (2007) Science 318:1266
6. Hanson MA, Cherezov V, Griffith MT, Roth CB, Jaakola VP, Chien EY, Velasquez J, Kuhn P, Stevens RC (2008) Structure 16:897
7. Warne T, Serrano-Vega MJ, Baker JG, Moukhametzianov R, Edwards PC, Henderson R, Leslie AG, Tate CG, Schertler GF (2008) Nature 454:486
8. Murakami M, Kouyama T (2008) Nature 453:363
9. Park JH, Scheerer P, Hofmann KP, Choe HW, Ernst OP (2008) Nature 454:183
10. Chien EY, Liu W, Zhao Q, Katritch V, Han GW, Hanson MA, Shi L, Newman AH, Javitch JA, Cherezov V, Stevens RC (2010) Science, 330:1091
11. Wu B, Chien EY, Mol CD, Fenalti G, Liu W, Katritch V, Abagyan R, Brooun A, Wells P, Bi FC, Hamel DJ, Kuhn P, Handel TM, Cherezov V, Stevens RC (2010) Science 330:1066
12. Jaakola VP, Ijzerman AP (2010) Curr Opin Struct Biol 20:401
13. Calleri E, Ceruti S, Cristalli G, Martini C, Temporini C, Parravicini C, Volpini R, Daniele S, Caccialanza G, Lecca D, Lambertucci C, Trincavelli ML, Marucci G, Wainer IW, Ranghino G, Fantucci P, Abbracchio MP, Massolini G (2010) J Med Chem 53:3489
14. Brink C (2003) Adv Exp Med Biol 525:7
15. Ciana P, Fumagalli M, Trincavelli ML, Verderio C, Rosa P, Lecca D, Ferrario S, Parravicini C, Capra V, Gelosa P, Guerrini U, Belcredito S, Cimino M, Sironi L, Tremoli E, Rovati GE, Martini C, Abbracchio MP (2006) EMBO J 25:4615
16. Pugliese AM, Trincavelli ML, Lecca D, Coppi E, Fumagalli M, Ferrario S, Failli P, Daniele S, Martini C, Pedata F, Abbracchio MP (2009) Am J Physiol Cell Physiol 297:C1028
17. Lecca D, Trincavelli ML, Gelosa P, Sironi L, Ciana P, Fumagalli M, Villa G, Verderio C, Grumelli C, Guerrini U, Tremoli E, Rosa P, Cuboni S, Martini C, Buffo A, Cimino M, Abbracchio MP (2008) PLoS One 3:e3579
18. Ceruti S, Villa G, Genovese T, Mazzon E, Longhi R, Rosa P, Bramanti P, Cuzzocrea S, Abbracchio MP (2009) Brain 132:2206
19. Chen Y, Wu H, Wang S, Koito H, Li J, Ye F, Hoang J, Escobar SS, Gow A, Arnett HA, Trapp BD, Karandikar NJ, Hsieh J, Lu QR (2009) Nat Neurosci 12:1398
20. Chenna R, Sugawara H, Koike T, Lopez R, Gibson TJ, Higgins DG, Thompson JD (2003) Nucleic Acids Res 31:3497

21. Eldesbrunner H, Facello M, Fu R, Liang J (1995) In: Proceedings of the 28th Hawaii international conference on systems science
22. Wojciechowski M, Lesyng B (2004) J. Phys. Chem. B 108:18368
23. Fumagalli M, Trincavelli L, Lecca D, Martini C, Ciana P, Abbracchio MP (2004) Biochem Pharmacol 68:113
24. Niv MY, Skrabanek L, Filizola M, Weinstein H (2006) J Comput Aided Mol Des 20:437
25. Costanzi S (2008) J Med Chem 51:2907
26. Katritch V, Jaakola VP, Lane JR, Lin J, Ijzerman AP, Yeager M, Kufareva I, Stevens RC, Abagyan R (2010) J Med Chem 53:1799
27. Peeters MC, van Westen GJ, Li Q, Ijzerman AP (2011) Trends Pharmacol Sci 32:35
28. Parravicini C, Abbracchio MP, Fantucci P, Ranghino G (2010) BMC Struct Biol 10:8
29. Parravicini C, Ranghino G, Abbracchio MP, Fantucci P (2008) BMC Bioinformatics 9:263
30. Frishman D, Argos P (1996) Protein Eng 9:133
31. Frishman D, Argos P (1997) Proteins 27:329
32. Thompson MJ, Goldstein RA (1997) Protein Sci 6:1963
33. Jones DT (1999) J Mol Biol 292:195
34. Cheng J, Randall AZ, Sweredoski MJ, Baldi P (2005) Nucleic Acids Res 33:W72
35. Globisch C, Pajeva IK, Wiese M (2008) ChemMedChem 3:280
36. Bondensgaard K, Ankersen M, Thogersen H, Hansen BS, Wulff BS, Bywater RP (2004) J Med Chem 47:888
37. Vilar S, Karpiak J, Costanzi S (2010) J Comput Chem 31:707
38. Eberini I, Rocco AG, Mantegazza M, Gianazza E, Baroni A, Vilardo MC, Donghi D, Galliano M, Beringhelli T (2008) J Mol Graph Model 26:1004
39. Eberini I, Fantucci P, Rocco AG, Gianazza E, Galluccio L, Maggioni D, Ben ID, Galliano M, Mazzitello R, Gaiji N, Beringhelli T (2006) Proteins 65:555
40. Ricchiuto P, Rocco AG, Gianazza E, Corrada D, Beringhelli T, Eberini I (2008) J Mol Recognit 21:348
41. Brink C, Dahlen SE, Drazen J, Evans JF, Hay DW, Nicosia S, Serhan CN, Shimizu T, Yokomizo T (2003) Pharmacol Rev 55:195
42. Melani A, Turchi D, Vannucchi MG, Cipriani S, Gianfriddo M, Pedata F (2005) Neurochem Int 47:442
43. Ciceri P, Rabuffetti M, Monopoli A, Nicosia S (2001) Br J Pharmacol 133:1323